

This article was downloaded by:

On: 23 January 2011

Access details: *Access Details: Free Access*

Publisher *Taylor & Francis*

Informa Ltd Registered in England and Wales Registered Number: 1072954 Registered office: Mortimer House, 37-41 Mortimer Street, London W1T 3JH, UK



Journal of Coordination Chemistry

Publication details, including instructions for authors and subscription information:

<http://www.informaworld.com/smpp/title~content=t713455674>

Crystal, molecular and electronic structure of $[\text{ReCl}_2(\eta^2\text{-N}_2\text{COPh-N',O})(\text{PPh}_3)_2]$

S. Michalik^a; B. Machura^a; R. Kruszynski^b; J. Kusz^c

^a Department of Inorganic and Coordination Chemistry, Institute of Chemistry, University of Silesia, 40-006 Katowice, Poland ^b Department of X-ray Crystallography and Crystal Chemistry, Institute of General and Ecological Chemistry, Lodz University of Technology, 90-924 Łódź, Poland ^c Institute of Physics, University of Silesia, 40-006 Katowice

To cite this Article Michalik, S. , Machura, B. , Kruszynski, R. and Kusz, J.(2008) 'Crystal, molecular and electronic structure of $[\text{ReCl}_2(\eta^2\text{-N}_2\text{COPh-N',O})(\text{PPh}_3)_2]$ ', *Journal of Coordination Chemistry*, 61: 7, 1066 – 1077

To link to this Article: DOI: 10.1080/00958970701484780

URL: <http://dx.doi.org/10.1080/00958970701484780>

PLEASE SCROLL DOWN FOR ARTICLE

Full terms and conditions of use: <http://www.informaworld.com/terms-and-conditions-of-access.pdf>

This article may be used for research, teaching and private study purposes. Any substantial or systematic reproduction, re-distribution, re-selling, loan or sub-licensing, systematic supply or distribution in any form to anyone is expressly forbidden.

The publisher does not give any warranty express or implied or make any representation that the contents will be complete or accurate or up to date. The accuracy of any instructions, formulae and drug doses should be independently verified with primary sources. The publisher shall not be liable for any loss, actions, claims, proceedings, demand or costs or damages whatsoever or howsoever caused arising directly or indirectly in connection with or arising out of the use of this material.

Crystal, molecular and electronic structure of [ReCl₂(η²-N₂COPh-N',O)(PPh₃)₂]

S. MICHALIK*†, B. MACHURA†, R. KRUSZYNSKI‡ and J. KUSZ§

†Department of Inorganic and Coordination Chemistry, Institute of Chemistry,
University of Silesia, 9th Szkolna St., 40-006 Katowice, Poland

‡Department of X-ray Crystallography and Crystal Chemistry, Institute of General
and Ecological Chemistry, Lodz University of Technology, 116 Zeromski St.,
90-924 Łódź, Poland

§Institute of Physics, University of Silesia, 4th Uniwersytecka St., 40-006 Katowice

(Received 17 February 2007; in final form 18 April 2007)

[ReO(OEt)Cl₂(PPh₃)₂] reacts with benzoylhydrazine in the presence of PPh₃ and hydrochloric acid to give [*N*-benzoylhydrazido(3-)-O,N']dichlorobis(triphenylphosphine) rhenium(V). The complex has been studied by IR, UV-Vis spectroscopy and X-ray crystallography. The molecular orbital diagram has been calculated with density functional theory (DFT). The spin-allowed singlet-singlet electronic transitions of [ReCl₂(η²-N₂COPh-N',O)(PPh₃)₂] have been calculated with the time-dependent DFT method, and the UV-Vis spectrum of the title compound has been discussed on this basis.

Keywords: Rhenium; Benzoylhydrazido complexes; X-ray structure; DFT calculations

1. Introduction

The success of the ¹⁸⁶Re(Sn)HEDEP (HEDEP = hydroksyethylenediphosphonic acid) radiopharmaceutical as a palliative of bone pain, has reawakened interest in the co-ordination chemistry of rhenium [1–3].

The [ReCl₂(η²-N₂COPh-N',O)(PPh₃)₂] complex has proven to be a key starting material for synthesis of dinitrogen and diazenido rhenium(I) complexes. The reactions of [ReCl₂(η²-N₂COPh-N',O)(PPh₃)₂] with neutral donor ligands such as acetonitrile, pyridine and pyrazole result in the opening of the chelate ring through displacement of the coordinated carbonyl group by the neutral donor ligands to give organodiazenido rhenium(I) complexes, [ReCl₂(N₂COPh)L(PPh₃)₂] [4, 5]. The refluxing of [ReCl₂(η²-N₂COPh-N',O)(PPh₃)₂] with mono- and di-tertiary phosphines in methanol gives high yields of dinitrogen Re(I) complexes, for example [ReCl(N₂)(CNMe){P(OMe)₃]₃ [6],

*Corresponding author. Email: smich1@wp.pl

$[\text{ReCl}(\text{N}_2)(\text{Et}_2\text{PCH}_2\text{CH}_2\text{PEt}_2)_2]$ [7] and $[\text{ReCl}(\text{N}_2)(\text{PMe}_2\text{Ph})_4]$ [8]. Chatt, Dilworth and Leigh reported the synthesis of $[\text{ReCl}_2(\eta^2\text{-N}_2\text{COPh-N',O})(\text{PPh}_3)_2]$ in 1971 [9]. However, the crystal and molecular structure of $[\text{ReCl}_2(\eta^2\text{-N}_2\text{COPh-N',O})(\text{PPh}_3)_2]$ has not been determined. Reports on this type of complex are sparse; the only structurally characterized chelated hydrazido(3-) rhenium(V) complexes appear to be $[\text{Re}(\eta^2\text{-NNC}(\text{SCH}_3)\text{S-N',O})(\text{L})(\text{PPh}_3)_2]$ $\text{H}_2\text{L} = S\text{-methyl}\beta\text{-N-}((2\text{-hydroxyphenyl})\text{ethyldene})\text{dithiocarbazate}$, $[\text{Re}(\eta^2\text{-NNC}(\text{SCH}_3)\text{S-N',O})\text{Cl}_2(\text{PPh}_3)_2]$ [10], and $[\text{ReCl}_2(\eta^2\text{-N}_2\text{COC}_6\text{H}_4\text{Cl-N',O})(\text{PPh}_3)_2]$ [11].

Here we present a modified synthesis, spectroscopic investigation, crystal, molecular and electronic structures of $[\text{ReCl}_2(\eta^2\text{-N}_2\text{COPh-N',O})(\text{PPh}_3)_2]$. The electronic structure of $[\text{ReCl}_2(\eta^2\text{-N}_2\text{COPh-N',O})(\text{PPh}_3)_2]$ has been calculated with density functional theory (DFT) and additional information about binding has been obtained by NBO analysis. Density functional theory (DFT) examines the electronic structure of transition metal complexes, meets the requirements of being accurate, easy to use and fast enough to allow the study of relatively large transition metal complexes [12]. The spin-allowed electronic transitions of $[\text{ReCl}_2(\eta^2\text{-N}_2\text{COPh-N',O})(\text{PPh}_3)_2]$ have been calculated with time-dependent DFT (TD-DFT), and the UV-V is spectrum of the title compound has been discussed on this basis. Recent calculations with TD-DFT for open- and closed-shell 5d-metal complexes (including rhenium complexes) have given good assignments of experimental spectra [13, 14].

2. Experimental

2.1. General procedure

All reagents used in the syntheses were commercially available and used without further purification. The $[\text{ReO}(\text{OEt})\text{Cl}_2(\text{PPh}_3)_2]$ was prepared according to the literature method [15], under argon.

The IR spectrum was recorded on a Nicolet Magna 560 spectrophotometer in the spectral range 4000–400 cm^{-1} with KBr pellets. Electronic spectrum was measured on a spectrophotometer Lab Alliance UV-Vis 8500 in the range 900–200 nm in dichloromethane. Elemental analyses (CHN) were performed on a Perkin-Elmer CHN-2400 analyzer.

2.2. Preparation of $[\text{ReCl}_2(\eta^2\text{-N}_2\text{COPh-N',O})(\text{PPh}_3)_2]$

$[\text{ReO}(\text{OEt})\text{Cl}_2(\text{PPh}_3)_2]$ (2 g, 2.4 mmol), concentrated hydrochloric acid (10 cm^3), benzoylhydrazine (2 g 14.7 mmol) and triphenylphosphine (2 g 7.6 mmol) were heated under reflux in 1 : 3 dichloromethane-ethanol (100 mL) for 20 min. The green crystalline precipitate was collected by filtration and crystals suitable for X-ray structure determination were obtained by recrystallization from toluene-ethanol. Yield 70%.

IR (KBr, cm^{-1}): 1482 (m), 1434 (vs), 1184 (m), 1163(vs), 1093 (vs), 746 (m), 693 (vs), 518 (vs), Calcd for $\text{C}_{43}\text{H}_{35}\text{Cl}_2\text{N}_2\text{OP}_2\text{Re}$: C 56.46%, H 3.86%, N 3.06%. Found: C 56%, H 4.8%, N 3.1%.

2.3. Crystal structures determination and refinement

A green crystal of $[\text{ReCl}_2(\eta^2\text{-N}_2\text{COPh-N',O})(\text{PPh}_3)_2]$ was mounted on a KM-4-CCD automatic diffractometer equipped with a CCD detector and used for data collection. X-ray intensity data were collected with graphite monochromated Mo-K α radiation ($\lambda = 0.71073 \text{ \AA}$) at 100(1) K. Details concerning crystal data and refinement are given in table 1. Lorentz, polarization and numerical absorption [16] were applied. The structure was solved by the Patterson method and subsequently completed by difference Fourier recycling. All the non-hydrogen atoms were refined anisotropically using full-matrix, least-squares. The hydrogen atoms were treated as “riding” on their parent carbon atoms and assigned isotropic temperature factors equal to 1.2 times the value of the equivalent temperature factor of the parent atom. SHELXS97 [17], SHELXL97 [18] and SHELXTL [19] programs were used for all the calculations.

3. Computational details

Gaussian03 [20] was used in the calculations. The geometry optimizations of $[\text{ReCl}_2(\eta^2\text{-N}_2\text{COPh-N',O})(\text{PPh}_3)_2]$ were carried out with the DFT method using the B3LYP functional [21, 22]. The electronic spectra of $[\text{ReCl}_2(\eta^2\text{-N}_2\text{COPh-N',O})(\text{PPh}_3)_2]$

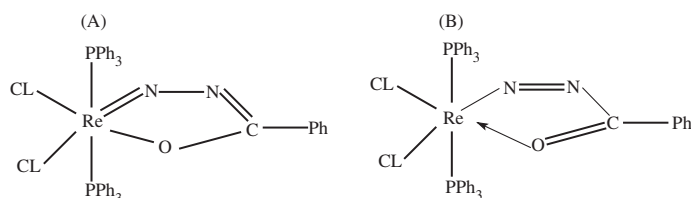
Table 1. Crystal data and structure refinement for $[\text{ReCl}_2(\eta^2\text{-N}_2\text{COPh-N',O})(\text{PPh}_3)_2]$.

Empirical formula	$\text{C}_{43}\text{H}_{35}\text{Cl}_2\text{N}_2\text{O}_2\text{P}_2\text{Re}$
Formula weight	914.77
Temperature (K)	100(1)
Wavelength (\AA)	0.71073
Crystal system	$P\bar{1}$
Space group	Triclinic
Unit cell dimensions	
a (\AA)	10.194(5)
b (\AA)	12.305(5)
c (\AA)	15.298(6)
α ($^\circ$)	93.63(3)
β ($^\circ$)	97.24(3)
γ ($^\circ$)	103.55(4)
Volume (\AA^3)	1842.1(14)
Z	2
Density (Calcd) (Mg m^{-3})	1.649
Absorption coefficient (mm^{-1})	3.568
$F(000)$	908
Crystal size (mm^3)	$0.30 \times 0.26 \times 0.06$
θ range for data collection ($^\circ$)	3.09 to 32.28
Index ranges	$-15 \leq h \leq 14$, $-18 \leq k \leq 18$, $-22 \leq l \leq 18$
Reflections collected	18742
Independent reflections	11965 ($R_{\text{int}} = 0.0268$)
Completeness to 2θ	0.812 and 0.349
Max. and min. transmission	99.8%
Data/restraints/parameters	11965/0/460
Goodness-of-fit on F^2	1.068
Final R indices [$I > 2\sigma(I)$]	$R_1 = 0.0450$, $wR_2 = 0.1002$
R indices (all data)	$R_1 = 0.0828$, $wR_2 = 0.1157$
Largest diff. peak and hole (e \AA^{-3})	1.249 and -1.104

were calculated with the TD-DFT method [23]. Calculations were performed by using ECP basis set on the rhenium atom, the standard 6-31+g** basis for chlorine, phosphorus, oxygen, and nitrogen, 6-31g* basis for carbon and 6-31G basis for hydrogen atoms. The Xe core electrons of Re were replaced by an effective core potential and DZ quality Hay and Wadt Los Alamos ECP basis set (LANL2DZ) [24] was used for the valence electrons. Additional *d* function with exponent $\alpha=0.3811$ and *f* function with exponent $\alpha=2.033$ on the rhenium atom were added. Natural bond orbital (NBO) calculations were performed with the NBO code [25] included in Gaussian03.

4. Results and discussion

The $[\text{ReCl}_2(\eta^2\text{-N}_2\text{COPh-N',O})(\text{PPh}_3)_2]$ complex was obtained from reaction of $[\text{ReO}(\text{OEt})\text{Cl}_2(\text{PPh}_3)_2]$ with benzoylhydrazine in the presence of PPh_3 and HCl . The elemental analysis of the complex is in good agreement with its formulation. The chelate ligand can coordinate as benzoylhydrazido(3-) (A) or benzoylhydrazido(1-) (B) (scheme 1) [9]:



Scheme 1. Coordination way of benzoylhydrazido ligand.

The lack of strong absorption bands assignable to $\nu(\text{C}=\text{O})$ or $\nu(\text{N}=\text{N})$ in the IR spectrum of $[\text{ReCl}_2(\eta^2\text{-N}_2\text{COPh-N',O})(\text{PPh}_3)_2]$ confirms the presence of the chelate benzoylhydrazido(3-) (A) [11]. The pair of bands at approximately 1434 and 1482 cm^{-1} are typical of coordinated triphenylphosphine [26].

4.1. Crystal structures

The $[\text{ReCl}_2(\eta^2\text{-N}_2\text{COPh-N',O})(\text{PPh}_3)_2]$ complex crystallizes in $P\bar{1}$ space group. The molecules are linked *via* weak intermolecular hydrogen bonds [27, 28], $\text{C}(11)\text{-H}(11)\cdots\text{Cl}(1)(1+x, y, z)$ with $\text{D}\cdots\text{A}$ distance 3.404(15) Å and $\text{D-H}\cdots\text{A}$ angle 122.3°. Intramolecular hydrogen bonds link $\text{C}(18)\text{-H}(18)\cdots\text{Cl}(2)$ with $\text{D}\cdots\text{A}$ distance 3.543(15) Å and $\text{D-H}\cdots\text{A}$ angle 150.1°; $\text{C}(12)\text{-H}(12)\cdots\text{N}(2)$ with $\text{D}\cdots\text{A}$ distance 3.393(19) Å and $\text{D-H}\cdots\text{A}$ angle 150.2° and $\text{C}(32)\text{-H}(32)\cdots\text{N}(2)$ with $\text{D}\cdots\text{A}$ distance 3.320(15) Å and $\text{D-H}\cdots\text{A}$ angle 139.0°, providing additional stabilization of $[\text{ReCl}_2(\eta^2\text{-N}_2\text{COPh-N',O})(\text{PPh}_3)_2]$. The ligand is planar in the range of experimental error (maximum deviation of 0.001(6) Å exists for C(37) atom) N_2CO moiety; the phenyl ring of (N_2COPh) is inclined at 21.1(6)° and also planar (maximum deviation of 0.008(9) Å exists for C(41) atom).

The molecular structure of $[\text{ReCl}_2(\eta^2\text{-N}_2\text{COPh-N',O})(\text{PPh}_3)_2]$ consists of discrete mononuclear species with the rhenium atom coordinated to *trans* phosphine ligands,

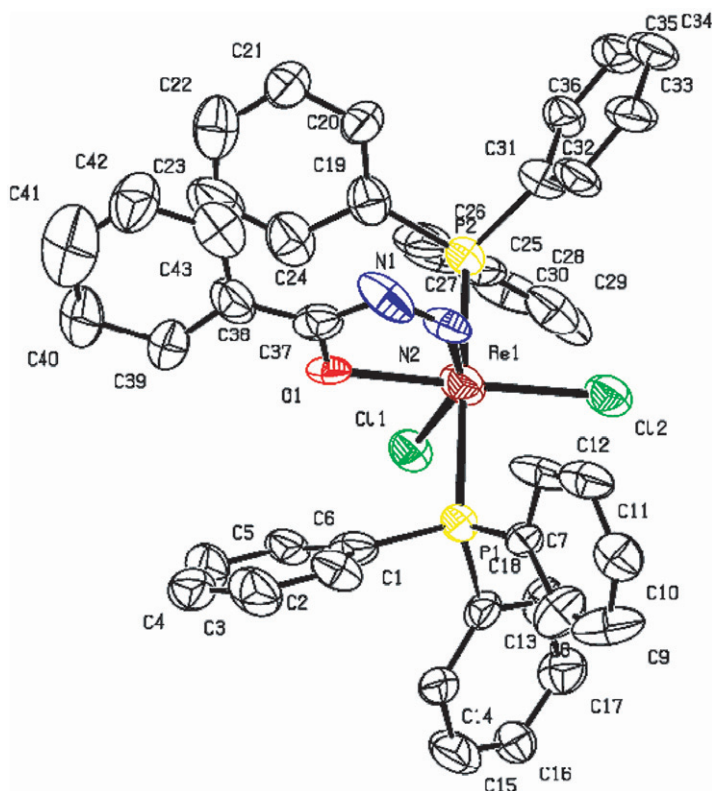


Figure 1. The molecular structure of $[\text{ReCl}_2(\eta^2\text{-N}_2\text{COPh-N',O})(\text{PPh}_3)_2]$.

chlorides *trans* to the nitrogen and carbonyl oxygen donors of the chelating benzoylhydrazone(3-) ligand, as shown in figure 1. The most important bond lengths and angles for $[\text{ReCl}_2(\eta^2\text{-N}_2\text{COPh-N',O})(\text{PPh}_3)_2]$ are reported in table 2. The $\text{Re}(1)\text{-N}(2)$ [1.819(9) Å] bond length is somewhat longer than found for $[\text{ReCl}_2(\eta^2\text{-N}_2\text{COC}_6\text{H}_4\text{Cl-N',O})(\text{PPh}_3)_2]$ [1.769(8) Å], whereas the $\text{N}(1)\text{-N}(2)$ [1.209(11) Å] distance is shorter than the corresponding distances for $[\text{ReCl}_2(\eta^2\text{-N}_2\text{COC}_6\text{H}_4\text{Cl-N',O})(\text{PPh}_3)_2]$ [1.30(2) Å] [11]. The $\text{Re}(1)\text{-O}(1)$ and $\text{C}(37)\text{-O}(1)$ bonds in $[\text{ReCl}_2(\eta^2\text{-N}_2\text{COPh-N',O})(\text{PPh}_3)_2]$ are typical for organohydrazone(3-) complexes of rhenium(V) [10, 11].

4.2. Geometry optimization

The geometry of $[\text{ReCl}_2(\eta^2\text{-N}_2\text{COPh-N',O})(\text{PPh}_3)_2]$ was optimized in a singlet state by the DFT method with the B3LYP functional. The optimized geometric parameters are gathered in table 2. The calculated bond lengths and angles are in agreement with the values based upon the X-ray crystal structure, and the general trends observed in the experimental data are well reproduced in the calculations.

4.3. Charge distribution

Table 3 presents the atomic charges from the Natural Population Analysis (NPA) for $[\text{ReCl}_2(\eta^2\text{-N}_2\text{COPh-N',O})(\text{PPh}_3)_2]$. The calculated charge on the rhenium is

Table 2. The experimental and calculated bond lengths (Å) and angles (°) for $[ReCl_2(\eta^2-N_2COPh-N',O)(PPh_3)_2]$.

	Experimental	Optimized
Re(1)–N(2)	1.819(9)	1.784
Re(1)–O(1)	2.165(6)	2.177
Re(1)–Cl(2)	2.351(3)	2.414
Re(1)–Cl(1)	2.360(3)	2.415
Re(1)–P(2)	2.448(3)	2.515
Re(1)–P(1)	2.464(3)	2.515
O(1)–C(37)	1.291(12)	1.274
C(37)–N(1)	1.356(14)	1.374
C(37)–C(38)	1.472(16)	1.468
N(1)–N(2)	1.209(11)	1.291
N(2)–Re(1)–O(1)	70.3(3)	70.6
N(2)–Re(1)–Cl(2)	105.8(3)	105.4
O(1)–Re(1)–Cl(2)	176.0(2)	1756.0
N(2)–Re(1)–Cl(1)	150.2(3)	151.0
O(1)–Re(1)–Cl(1)	80.1(2)	80.4
Cl(2)–Re(1)–Cl(1)	103.81(10)	103.6
N(2)–Re(1)–P(2)	90.3(3)	94.0
O(1)–Re(1)–P(2)	90.64(19)	92.7
Cl(2)–Re(1)–P(2)	89.87(10)	92.6
Cl(1)–Re(1)–P(2)	86.51(10)	87.2
N(2)–Re(1)–P(1)	96.2(3)	94.0
O(1)–Re(1)–P(1)	89.96(19)	92.6
Cl(2)–Re(1)–P(1)	89.99(10)	87.5
Cl(1)–Re(1)–P(1)	86.99(10)	87.2
P(2)–Re(1)–P(1)	173.27(10)	171.6
C(7)–P(1)–Re(1)	117.1(4)	116.5
C(13)–P(1)–Re(1)	115.6(4)	114.9
C(1)–P(1)–Re(1)	111.3(4)	111.9
C(19)–P(2)–Re(1)	110.4(3)	111.8
C(31)–P(2)–Re(1)	115.9(4)	114.9
C(25)–P(2)–Re(1)	116.3(4)	116.6
C(37)–O(1)–Re(1)	110.1(7)	112.2
O(1)–C(37)–N(1)	118.2(10)	122.2
O(1)–C(37)–C(38)	118.7(11)	117.3
N(1)–C(37)–C(38)	123.1(11)	120.5
N(2)–N(1)–C(37)	106.6(10)	105.7
N(1)–N(2)–Re(1)	134.6(8)	134.3

Table 3. Atomic charges from the natural population analysis (NPA) for $[ReCl_2(\eta^2-N_2COPh-N',O)(PPh_3)_2]$.

Atom	Charge
Re(1)	0.345
Cl(1)	–0.401
Cl(2)	–0.351
N(1)	–0.389
N(2)	–0.170
O(1)	–0.608
P(1)	1.377
P(2)	1.377
C(37)	0.628
C(38)	–0.136

Table 4. The occupancies and hybridization of the calculated natural bond orbitals (NBOs) between the rhenium and the chelate ring for $[\text{ReCl}_2(\eta^2\text{-N}_2\text{COPh-N',O})(\text{PPh}_3)_2]$.

BD	Occupancy	Hybridization of NBO	BD*	Occupancy
Re–N(2)	1.969	$0.623(\text{d})_{\text{Re}} + 0.783(\text{p})_{\text{O}}$	$0.783(\text{d})_{\text{Re}} - 0.623(\text{p})_{\text{O}}$	0.290
	1.922	$0.751(\text{d})_{\text{Re}} + 0.661(\text{p})_{\text{O}}$	$0.661(\text{d})_{\text{Re}} - 0.751(\text{p})_{\text{O}}$	0.491
N(1)–N(2)	1.983	$0.699(\text{sp}^{2.47})_{\text{N}(1)} + 0.715(\text{sp}^{2.20})_{\text{N}(2)}$	$0.715(\text{sp}^{2.47})_{\text{N}(1)} - 0.699(\text{sp}^{2.20})_{\text{N}(2)}$	0.014
N(1)–C(37)	1.972	$0.639(\text{sp}^{2.18})_{\text{C}(37)} + 0.769(\text{sp}^{2.05})_{\text{N}(1)}$	$0.769(\text{sp}^{2.18})_{\text{C}(37)} - 0.639(\text{sp}^{2.05})_{\text{N}(1)}$	0.057
	1.688	$0.547(\text{p})_{\text{C}(37)} + 0.837(\text{p})_{\text{N}(1)}$	$0.837(\text{p})_{\text{C}(37)} - 0.547(\text{p})_{\text{N}(1)}$	0.466
O(1)–C(37)	1.992	$0.816(\text{sp}^{1.57})_{\text{O}(1)} + 0.578(\text{sp}^{2.31})_{\text{C}(37)}$	$0.578(\text{sp}^{1.57})_{\text{O}(1)} - 0.816(\text{sp}^{2.31})_{\text{C}(37)}$	0.028

BD denotes 2-center bond, * –denotes antibond NBO.

considerably lower than the formal charge of +5. The populations of the $5d_{xy}$, $5d_{xz}$, $5d_{yz}$, $5d_{x^2-y^2}$ and $5d_{z^2}$ orbitals of the central atom $[\text{ReCl}_2(\eta^2\text{-N}_2\text{COPh-N',O})(\text{PPh}_3)_2]$ are as follows: 1.597, 1.636, 0.921, 1.077 and 0.953, resulting from significant charge donation from the ligands. The P atoms are positively charged and the charges on the oxygen and nitrogen atoms of the chelate ligand are significantly smaller than –1 and –2, respectively. Some differences in values of charges are observed for the chloride ligands – less negative is chloride in the *trans* position to the oxygen atom of the chelate ligand, indicating higher electron density delocalization from Cl(2) ion towards the rhenium center consistent with differences in the Re–Cl bond lengths.

4.4. NBO analysis

Table 4 presents the occupancies and hybridization of the calculated natural bond orbitals (NBOs) in the $\text{Re}(\eta^2\text{-N}_2\text{COPh-N',O})$ unit.

Each natural bond orbital (NBO) σ_{AB} can be written in terms of two directed valence hybrids (HHOs) h_A i h_B on atoms A and B:

$$\sigma_{AB} = c_A h_A + c_B h_B$$

where c_A i c_B are polarization coefficients. Each valence bonding NBO must in turn be paired with a corresponding valence *anti*-bonding NBO,

$$\sigma^*_{AB} = c_B h_A - c_A h_B$$

to complete the span of the valence space. The Lewis-type (donor) NBOs are thereby complemented by the non-Lewis-type (acceptor) NBOs that are formally empty in an idealized Lewis picture. Interactions between ‘filled’ Lewis-type NBOs and ‘empty’ non-Lewis NBOs lead to loss of occupancy from the localized NBOs of the idealized Lewis structure into the empty non-Lewis orbitals, referred to as ‘delocalization’ corrections to the zeroth-order natural Lewis structure [29].

The rhenium–nitrogen interaction in $[\text{ReCl}_2(\eta^2\text{-N}_2\text{COPh-N',O})(\text{PPh}_3)_2]$ can be described as a triple bond. The detected natural Re(1)–N(2) bond orbitals of $[\text{ReCl}_2(\eta^2\text{-N}_2\text{COPh-N',O})(\text{PPh}_3)_2]$ are of π character - the p_z and p_y oxygen orbitals and d_{yz} and d_{xy} rhenium orbitals are involved in their formation. Not detected $\sigma_{\text{Re}(1)\text{-N}(2)}$ bond has character of predominant Coulomb-type interactions between the central ion and organohydrazido(3–) ligand [30]. The N(1)–C(37) bond is double in

character, whereas the N(1)–N(2) and C(37)–O(1) correspond to single bonds. The Re(1)–O(1) bond, similar to the Re(1)–N(2) bond, is ionic in character. Accordingly, the NBO analysis confirms the presence of the benzoylhydrazido(3–) ligand (molecule A in scheme) in the coordination sphere of the title complex.

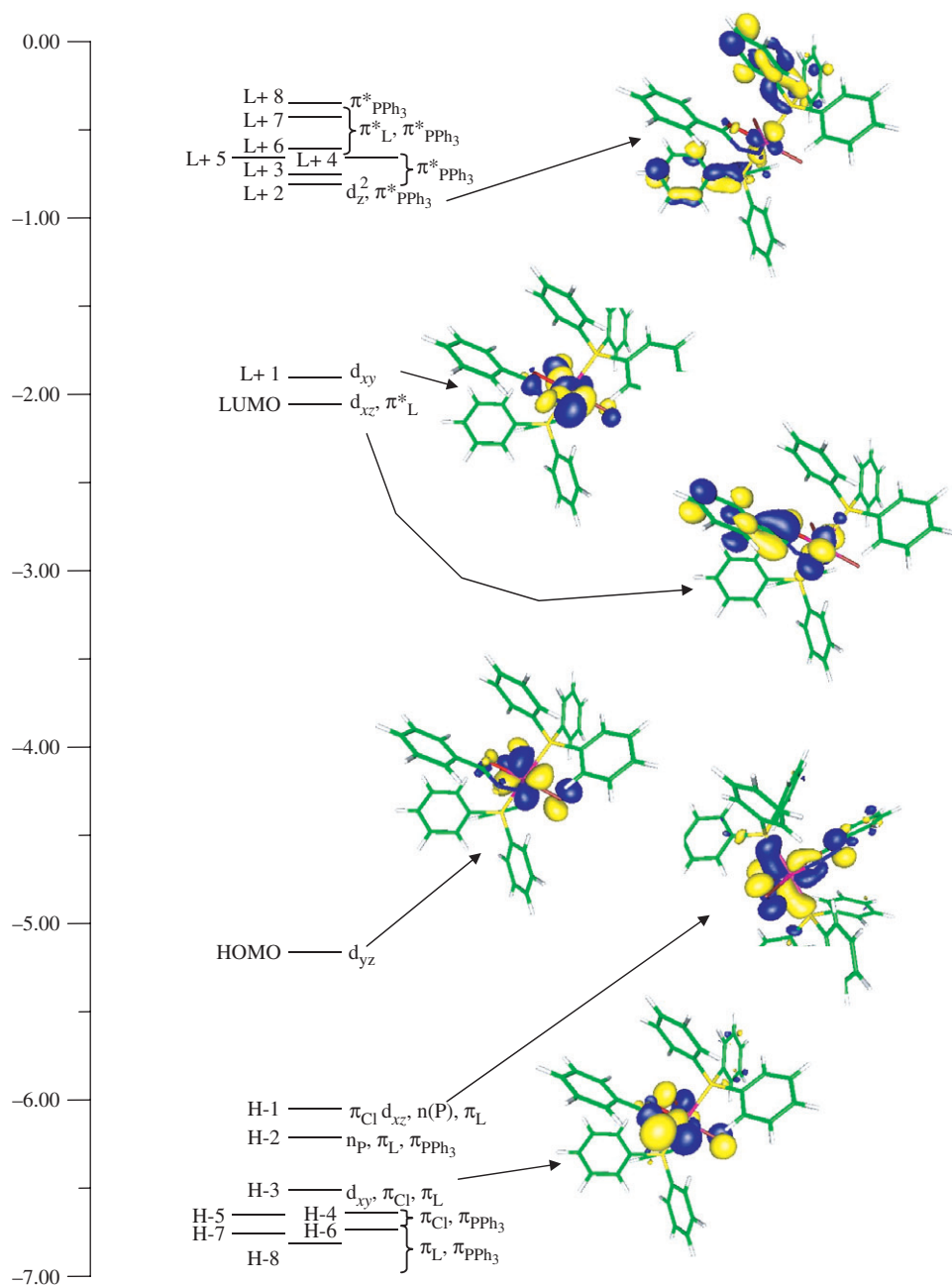


Figure 2. The energy (eV), character and some contours of the unoccupied and occupied molecular orbitals of $[\text{ReCl}_2(\eta^2\text{-N}_2\text{COPh-N',O})(\text{PPh}_3)_2]$.

4.5. Electronic structure

The energies, characters and contours of several lowest unoccupied molecular orbitals (LUMO or L) and highest occupied molecular orbitals (HOMO or H) of $[\text{ReCl}_2(\eta^2\text{-N}_2\text{COPh-N',O})(\text{PPh}_3)_2]$ are presented in figure 2. The HOMO–LUMO gap is 3.11 eV. The highest occupied MO of $[\text{ReCl}_2(\eta^2\text{-N}_2\text{COPh-N',O})(\text{PPh}_3)_2]$ is of d_{yz} type with antibonding contributions from p_π chlorine and oxygen orbitals. The remaining four d-type orbitals of rhenium are found among unoccupied MOs, confirming d^2 configuration of the rhenium.

The rhenium atom uses six valence orbitals, $5d_{x^2-y^2}$, $5d_{z^2}$, $6s$, $6p_x$, $6p_y$ and $6p_z$ to form σ -bonds with the six ligands, the occupied $5d_{yz}$ orbital of Re remains nonbonding, and empty $5d_{xz}$ and $5d_{xy}$ orbitals interact with the filled $2p_z$ and $2p_y$ orbitals of the nitrogen atom of the benzoylhydrazido(3-) ligand to give two π -bonding and two π -antibonding molecular orbitals. The $\pi_{\text{Re-N}}$ bonding interaction makes the largest contribution into the H-1 and H-3 orbitals. The LUMO and LUMO + 1 are closely spaced in energy and can be ascribed as π -antibonding rhenium–nitrogen of the benzoylhydrazido(3-) molecular orbitals.

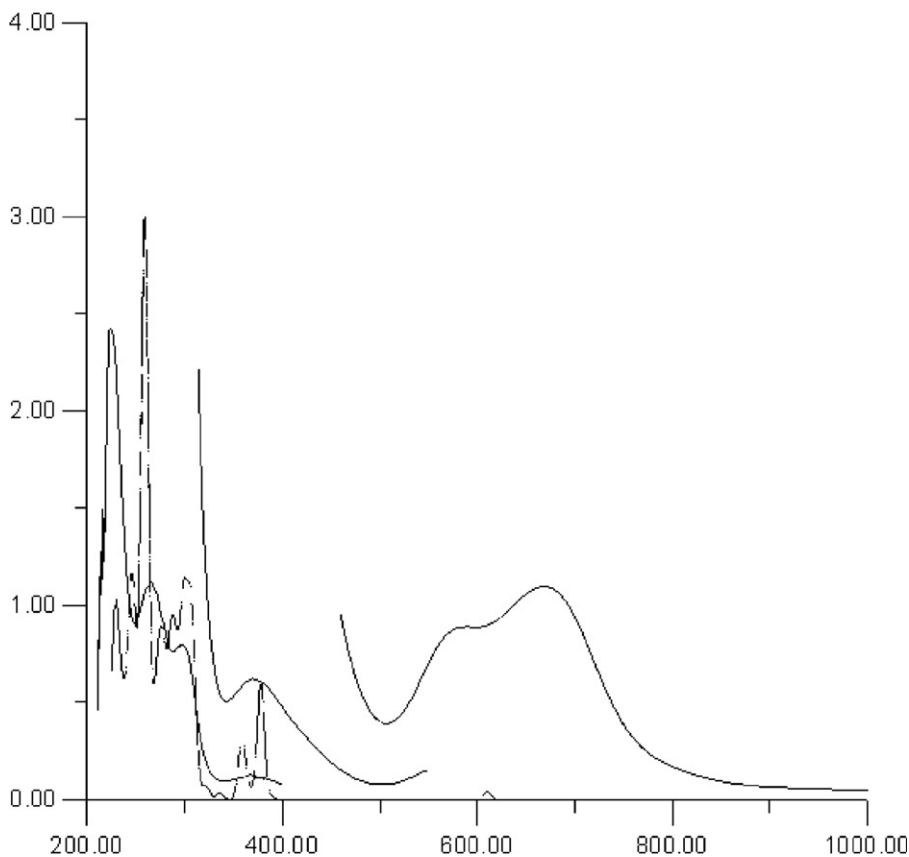


Figure 3. The experimental (—) and calculated (---) electronic absorption spectrum of $[\text{ReCl}_2(\eta^2\text{-N}_2\text{COPh-N',O})(\text{PPh}_3)_2]$.

4.6. Electronic spectrum

The experimental and calculated electronic spectra of $[\text{ReCl}_2(\eta^2\text{-N}_2\text{COPh-N',O})(\text{PPh}_3)_2]$ are presented in figure 3. Each calculated transition is represented by a Gaussian function $y = ce^{-bx^2}$ with the height (c) equal to the oscillator strength and b equal to 0.04 nm^{-2} .

Table 5 shows the spin-allowed singlet-singlet electronic transitions calculated with the TD-DFT method for $[\text{ReCl}_2(\eta^2\text{-N}_2\text{COPh-N',O})(\text{PPh}_3)_2]$. For the high energy part of the spectrum, only transitions with oscillator strengths larger than 0.0100 are listed in table 5.

The two longest wavelength experimental bands at 671.0 and 591.2 nm are attributed to the transition of $d \rightarrow d$ character with small oscillator strengths calculated at 702.8 and 610.3 nm, respectively.

Table 5. The energy and molar absorption coefficients of experimental absorption bands and the electronic transitions calculated with the TD-DFT method for $[\text{ReCl}_2(\eta^2\text{-N}_2\text{COPh-N',O})(\text{PPh}_3)_2]$.

The most important orbital excitations	Character	λ (nm)	E (eV)	f	Experimental $\Lambda(\text{nm})(E[\text{eV}])\epsilon$
H \rightarrow L + 1	d \rightarrow d	702.8	1.76	0.0001	671.0(1.85) 394
H \rightarrow L	d \rightarrow d	610.3	2.03	0.0042	591.2(2.10) 320
H-1 \rightarrow L	$\pi(\text{Cl})/\pi(\text{L}) \rightarrow$ d	377.9	3.28	0.0661	381.0 (3.25) 3 625
H-2 \rightarrow L	$\pi(\text{L})/\pi(\text{PPh}_3)/n(\text{P}) \rightarrow$ d	357.9	3.46	0.0284	
H \rightarrow L + 15	d \rightarrow d	311.5	3.98	0.0085	
H \rightarrow L + 7	d \rightarrow $\pi^*(\text{L})/\pi^*(\text{PPh}_3)$	310.4	3.99	0.0188	
H-4 \rightarrow L + 1	$\pi(\text{PPh}_3)/\pi(\text{Cl}) \rightarrow$ d	305.9	4.05	0.0842	296.5 (4.18) 47250
H-4 \rightarrow L + 1	$\pi(\text{PPh}_3)/\pi(\text{Cl}) \rightarrow$ d	301.3	4.11	0.0279	
H-7 \rightarrow L	$\pi(\text{PPh}_3)/\pi(\text{L}) \rightarrow$ d				
H-7 \rightarrow L	$\pi(\text{PPh}_3)/\pi(\text{L}) \rightarrow$ d	298.2	4.16	0.0796	
H-6 \rightarrow L + 1	$\pi(\text{PPh}_3) \rightarrow$ d	291.2	4.26	0.0406	
H-8 \rightarrow L + 1	$\pi(\text{PPh}_3)/\pi(\text{L}) \rightarrow$ d	287.8	4.31	0.0303	
H-12 \rightarrow L	$\pi(\text{PPh}_3)/\pi(\text{Cl}) \rightarrow$ d	285.1	4.35	0.0239	
H \rightarrow L + 10	d \rightarrow $\pi^*(\text{PPh}_3)$				
H-14 \rightarrow L	$\pi(\text{PPh}_3)/\pi(\text{L}) \rightarrow$ d	283.7	4.37	0.0215	
H-12 \rightarrow L	$\pi(\text{PPh}_3)/\pi(\text{Cl}) \rightarrow$ d				
H-1 \rightarrow L + 2	$\pi(\text{Cl})/\pi(\text{L}) \rightarrow$ d/ $\pi^*(\text{PPh}_3)$	277.6	4.47	0.0562	
H \rightarrow L + 11	d \rightarrow $\pi^*(\text{PPh}_3)$	274.5	4.52	0.0109	
H-16 \rightarrow L	$\pi(\text{PPh}_3)/\pi(\text{L}) \rightarrow$ d	271.9	4.56	0.0514	265.0 (4.68) 64060
H-17 \rightarrow L + 1	$\pi(\text{Cl}) \rightarrow$ d	265.1	4.68	0.0101	
H-1 \rightarrow L + 5	$\pi(\text{Cl})/\pi(\text{L}) \rightarrow$ $\pi^*(\text{PPh}_3)$	261.2	4.75	0.0456	
H \rightarrow L + 17	d \rightarrow d/ $\pi^*(\text{PPh}_3)$	259.9	4.77	0.0208	
H-1 \rightarrow L + 4	$\pi(\text{Cl})/\pi(\text{L}) \rightarrow$ $\pi^*(\text{PPh}_3)$	258.9	4.79	0.0155	
H-2 \rightarrow L + 2	$\pi(\text{PPh}_3)/\pi(\text{L}) \rightarrow$ d/ $\pi^*(\text{PPh}_3)$	258.5	4.80	0.2496	
H-1 \rightarrow L + 6	$\pi(\text{Cl})/\pi(\text{L}) \rightarrow$ $\pi^*(\text{PPh}_3)/\pi^*(\text{L})$	255.0	4.86	0.0141	
H-2 \rightarrow L + 4	$\pi(\text{PPh}_3)/\pi(\text{L}) \rightarrow$ $\pi^*(\text{PPh}_3)$	248.3	4.99	0.0298	
H-2 \rightarrow L + 9	$\pi(\text{PPh}_3)/\pi(\text{L}) \rightarrow$ $\pi^*(\text{PPh}_3)$	245.9	5.04	0.0634	
H-19 \rightarrow L	$\pi(\text{Cl}) \rightarrow$ d	238.5	5.20	0.0113	
H-2 \rightarrow L + 9	$\pi(\text{PPh}_3)/\pi(\text{L}) \rightarrow$ $\pi^*(\text{PPh}_3)$				
H-1 \rightarrow L + 9	$\pi(\text{Cl})/\pi(\text{L}) \rightarrow$ $\pi^*(\text{PPh}_3)$				
H-4 \rightarrow L + 3	$\pi(\text{PPh}_3)/\pi(\text{Cl}) \rightarrow$ $\pi^*(\text{PPh}_3)$	231.9	5.35	0.0240	225.4(5.50) 160010
H-7 \rightarrow L + 2	$\pi(\text{PPh}_3)/\pi(\text{L}) \rightarrow$ d/ $\pi^*(\text{PPh}_3)$	228.2	5.43	0.0182	
H-2 \rightarrow L + 8	$\pi(\text{PPh}_3)/\pi(\text{L}) \rightarrow$ $\pi^*(\text{PPh}_3)$				
H-6 \rightarrow L + 3	$\pi(\text{PPh}_3) \rightarrow$ $\pi^*(\text{PPh}_3)$	228.0	5.44	0.0381	
H-6 \rightarrow L + 3	$\pi(\text{PPh}_3) \rightarrow$ $\pi^*(\text{PPh}_3)$	227.5	5.45	0.0160	

ϵ – molar absorption coefficient [$\text{dm}^3 \text{ mol}^{-1} \text{ cm}^{-1}$], f – oscillator strength, H – highest occupied molecular orbital, L – lowest unoccupied molecular orbital.

The absorption bands at 381 and 296.5 nm are assigned to the *Ligand–Metal Charge Transfer* occurring from the benzoylhydrazido(3-), PPh₃ and chloride ligands to the rhenium d orbitals. The experimental band at 265.0 nm is attributed to the *Ligand–Metal Charge Transfer* and *Ligand–Ligand Charge Transfer* calculated in the range 278–255 nm. The shortest wavelength experimental band at 225.4 results from the *Ligand–Ligand Charge Transfer* and interligand (*IL*) transitions.

Supplementary data

Supplementary data for C₇H₈N₄Cl₃ORe are available from the CCDC, 12 Union Road, Cambridge CB2 1EZ, UK on request, quoting the deposition number 636274.

Acknowledgements

The Gaussian03 calculations were carried out in the Wrocław Centre for Networking and Supercomputing, WCSS, Wrocław, Poland.

References

- [1] A. Lazzaro, G. Vertuani, P. Bergamini, N. Mantovani, A. Marchi, L. Marvelli, R. Rossi, V. Bertolasi, V. Ferretti. *J. Chem. Soc., Dalton Trans.*, 2843 (2002).
- [2] E.G. Garayoa, D. Rüegg, P. Bläuenstein, M. Zwimpfer, I.U. Khan, V. Maes, A. Blanc, A.G. Beck-Sickinger, D.A. Tourwé, P.A. Schubinger. *Nucl. Med. Biol.*, **34**, 17 (2007).
- [3] A.R. Cowley, J.R. Dilworth, P.S. Donnelly, S.J. Ross. *J. Chem. Soc., Dalton Trans.*, 78 (2007).
- [4] L. Marvelli, N. Mantovani, A. Marchi, R. Rossi, M. Brugnati, P. Barbaro, I. de los Rios, V. Bertolasi. *J. Chem. Soc., Dalton Trans.*, 713 (2004).
- [5] J.O. Dziegielewski, S. Michalik, R. Kruszyński, T.J. Bartczak, J. Kusz. *Polyhedron*, **22**, 3307 (2003).
- [6] M. Fernanda, N.N. Carvalho, J.L. Pombeiro, U. Schubert, O. Orama, C.J. Pickett, R.L. Richards. *J. Chem. Soc., Dalton Trans.*, 2079 (1985).
- [7] J. Chatt, W. Hussain, G.F. Leigh, H.M. Ali, C.J. Pickett, D.A. Rankin. *J. Chem. Soc., Dalton Trans.*, 1131 (1985).
- [8] J. Chatt, J.R. Dilworth, G.J. Leigh. *J. Chem. Soc. A*, 612 (1973).
- [9] J. Chatt, J.R. Dilworth, G.J. Leigh, V.D. Gupta. *J. Chem. Soc. A*, 2631 (1971).
- [10] F. Mévellec, N. Lepareur, A. Roucoux, N. Noiret, H. Patin, G. Bandoli, M. Porchia, F. Tisato. *Inorg. Chem.*, **41**, 1591 (2002).
- [11] T. Nicholson, J. Zubieta. *Polyhedron*, **7**, 171 (1998).
- [12] H. Chermette. *Coord. Chem. Rev.*, **699**, 178 (1998).
- [13] M.C. Aragoni, M. Arca, T. Cassano, C. Denotti, F.A. Devillanova, F. Isaia, V. Lippolis, D. Natali, L. Niti, M. Sampietro, R. Tommasi, G. Verani. *Inorg. Chem. Commun.*, **5**, 869 (2002).
- [14] P. Romaniello, F. Lej. *Chem. Phys. Lett.*, **372**, 51 (2003).
- [15] J. Chatt, J.R. Dilworth, G.J. Leigh. *J. Chem. Soc. A*, 2239 (1970).
- [16] CrysAlis RED, Oxford Diffraction Ltd., Version 1.171.29.2.
- [17] G.M. Sheldrick. *Acta Cryst.*, **A46**, 467 (1990).
- [18] G.M. Sheldrick. *SHELXL97. Program for the Solution and Refinement of Crystal Structures*, University of Göttingen, Germany (1997).
- [19] G.M. Sheldrick. *SHELXTL: release 4.1*, Siemens Crystallographic Research Systems (1990).
- [20] Gaussian 03, Revision B.03, M.J. Frisch, G.W. Trucks, H.B. Schlegel, G.E. Scuseria, M.A. Robb, J.R. Cheeseman, J.A. Montgomery Jr, T. Vreven, K.N. Kudin, J.C. Burant, J.M. Millam, S.S. Iyengar, J. Tomasi, V. Barone, B. Mennucci, M. Cossi, G. Scalmani, N. Rega, G.A. Petersson, H. Nakatsuji, M. Hada, M. Ehara, K. Toyota, R. Fukuda, J. Hasegawa, M. Ishida, T. Nakajima, Y. Honda, O. Kitao,

- H. Nakai, M. Klene, X. Li, J.E. Knox, H.P. Hratchian, J.B. Cross, C. Adamo, J. Jaramillo, R. Gomperts, R.E. Stratmann, O. Yazyev, A.J. Austin, R. Cammi, C. Pomelli, J.W. Ochterski, P.Y. Ayala, K. Morokuma, G.A. Voth, P. Salvador, J.J. Dannenberg, V.G. Zakrzewski, S. Dapprich, A.D. Daniels, M.C. Strain, O. Farkas, D.K. Malick, A.D. Rabuck, K. Raghavachari, J.B. Foresman, J.V. Ortiz, Q. Cui, A.G. Baboul, S. Clifford, J. Cioslowski, B.B. Stefanov, G. Liu, A. Liashenko, P. Piskorz, I. Komaromi, R.L. Martin, D.J. Fox, T. Keith, M.A. Al-Laham, C.Y. Peng, A. Nanayakkara, M. Challacombe, P.M.W. Gill, B. Johnson, W. Chen, M.W. Wong, C. Gonzalez, J.A. Pople. Gaussian, Inc., Pittsburgh, PA (2003).
- [21] A.D. Becke. *J. Chem. Phys.*, **98**, 5648 (1993).
- [22] C. Lee, W. Yang, R.G. Parr. *Phys. Rev.*, **B37**, 785 (1988).
- [23] M.E. Casida, In *Recent Developments and Applications in Modern Density Functional Theory*, Theoretical and Computational Chemistry, J.M. Seminario (Ed.), Vol. 4, Elsevier, Amsterdam (1996).
- [24] P.J. Hay, W.R. Wadt. *J. Chem. Phys.*, **82**, 299 (1985).
- [25] E.D. Glendening, A.E. Reed, J.E. Carpenter, F. Weinhold. NBO (version 3.1).
- [26] S. Michalik, J.O. Dzięgielewski, R. Kruszyński. *J. Coord. Chem.*, **58**, 1493 (2005).
- [27] G.A. Jeffrey, W. Saenger. *Hydrogen Bonding in Biological Structures*, Springer-Verlag, Berlin (1994).
- [28] G.R. Desiraju, T. Steiner. *The Weak Hydrogen Bond in Structural Chemistry and Biology*, Oxford University Press (1999).
- [29] A.E. Reed, L.A. Curtiss, F. Weinhold. *Chem. Rev.*, **88**, 899 (1988).
- [30] M.L. Kuznestov, A.J.L. Pombeiro. *J. Chem. Soc., Dalton Trans.*, 738 (2003).